



Politecnico di Bari

Repository Istituzionale dei Prodotti della Ricerca del Politecnico di Bari

Towards patient dose optimization in digital radiography

This is a pre-print of the following article

Original Citation:

Towards patient dose optimization in digital radiography / Andria, Gregorio; Attivissimo, Filippo; Guglielmi, G.; Lanzolla, Anna Maria Lucia; Maiorana, A.; Mangiantini, M.. - In: MEASUREMENT. - ISSN 0263-2241. - 79:(2016), pp. 331-338. [10.1016/j.measurement.2015.08.015]

Availability:

This version is available at <http://hdl.handle.net/11589/5556> since: 2021-03-10

Published version

DOI:10.1016/j.measurement.2015.08.015

Terms of use:

(Article begins on next page)

Towards patient dose optimization in digital radiography

G. Andria¹, F. Attivissimo¹, G. Guglielmi^{2,3}, A.M.L. Lanzolla¹, A. Maiorana²,
M. Mangiantini²,

¹*Department of Electrical and Information Engineering (DEI), Polytechnic of Bari*
[andria ,attivissimo, lanzolla]@misura.poliba.it

²*Department of Medical Physics, Scientific Institute Hospital "Casa Sollievo della Sofferenza"*
[a.maiorana ,m.mangiantini]@operapadrepio.it

³*Department of Radiology, University of Foggia*
giuseppe.guglielmi@unifg.it

Abstract— Digital radiographic imaging systems cover a wide range of clinical applications and can produce adequate image quality using a broad span of exposure levels. Over exposure may generate higher dose levels without an effective increasing of the images quality; thus experimental data analysis is an ongoing process useful to provide information about adequacy of radiation exposure. The main purpose of this work is the assessment of quality performance of medical imaging systems by using objective image quality tests. To this aim, the influence of radiographic parameters has been investigated in order to reduce radiation dose to patients by assuring a good quality of the images.

Keywords—Biomedical x-ray imaging, image quality, phantom, image contrast, radiation dose.

I. INTRODUCTION

Medical imaging systems are widely used in radiological diagnosis. Their main benefits are more accurate and faster exams, elimination of exploratory surgery, availability of post processing and computed aided detection, immediate images availability, and ability to store and/or transmit the images electronically [1], [2]. Opposite, the potential risk of associated ionization radiation exposure from medical imaging, such as Computed Tomography and digital radiography [3] must be considered in risk to benefit ratio assessment.

Growing concern expressed by Radiology Community about the increasing exposure to ionizing radiation, has led to investigate and develop suitable strategies able to deliver the lowest dose necessary to provide sufficient image quality required to extract the desiderate details and diagnostic information.

Many studies have been proposed about the performance comparison of an imaging system with another “reference” system to define the amount of possible maximum radiation dose reduction without affecting the reference image quality. Using this approach, it is possible to optimize the system performance by means of an appropriate selection of technical parameters [4]-[7]. Moreover, to assure a correct use of digital x-ray devices in clinical practice, it is necessary to perform regularly standardized quality control tests developed both to detect possible image quality degradation and to allow corrective actions on the analyzed device [12].

In this work, suitable and objective tests for image quality evaluation have been performed by identifying the main parameters influencing the radiographic performance.

II. IMAGE QUALITY IN DIAGNOSTIC RADIOLOGY

The goal in optimizing image quality is to provide images able to ensure an adequate contrast details with the minimum radiation dose to the patient.

In digital radiographic systems three main parameters affect the image quality: (i) the *tube voltage* representing the penetration energy of the photon in x-ray tube, (ii) the *tube current* linked to the quantity of photons generated in the tube, (iii) the *exposure time* expressing the emission time of the radiation beam (i.e. an increase in time provides higher exposure).

The suitable setting of these parameters directly affects the diagnostic results. There is a wide variety of approaches in the assessment of radiological image quality [5]-[11]. The most applied techniques are based on the use of *Test Objects*, consisting on a set of standard objects able to provide objective information about the capability of imaging system under test and to distinguish details at different contrast and resolution values under specific conditions [7]-[9].

Alternative methods for image quality evaluation use anthropomorphic phantoms based on suitable model for simulating the tissue composition of human body [12], [13]. Their aim should be to reproduce as closely as possible the behavior of x-ray energy after passing through structures of standard sized patients. These phantoms are systems complex and expensive and are unlikely available in all departments of radiology.

The identification of an objective measurement index for image quality assessment is a very crucial issue which has led many researchers to develop and propose different quality metrics whose effectiveness depends on image characteristics and specific applications [14]- [17]. In radiological diagnosis the image contrast is a very important factor which allows to distinguish the anatomical structures of interest from their

surrounding and then it is of very basic importance for the correctness of the medical exams.

Another important factor is the resolution including the capability to distinguish different adjacent structures.

For these reasons the quality indexes taking into account resolution and contrast are mainly used in the radiological quality assessment.

III. MATERIALS AND METHOD

In the proposed study, Test Objects were applied to evaluate the performance of a digital radiographic system; particularly, the KODAK DIRECTVIEW DR 7500 [14] device, used for routine radiographies in Hospital “Casa Sollievo della Sofferenza” (San Giovanni Rotondo, Italy) is been used in the tests. The tested device is equipped with an *Automatic Exposure Control* device (AEC) [18], [19], which automatically sets the x-ray parameters as function of the selected beam potential so in order to keep approximately constant the exposure value. It has antiscatter grid placed close to the entrance surface of an image receptor to reduce the amount of scattered radiation reaching the receptor, according to the European Guidelines for quality assurance in x-ray diagnosis [20].

A X-RAY DEVICE ANALYSIS

As first step, the characterization of analysed radiographic device has been carried out. In particular, the x-ray output intensity expressed as absorbed dose to air (*Air-Kerma* - K_{air} -) [9] was evaluated as function of tube voltage (V) and of the tube current and exposure time product, often referred as the *tube loading* (Q).

Several studies have proved that K_{air} is linearly dependent on the tube loading and approximately proportional on the square of the tube voltage [21], [22].

For this aim several experimental tests have been carried to measure the *Air-Kerma* at a focus-to-detector distance of 2 m by using a RTI Piranha dosimeter [23] and by varying the values of x-ray parameters in the range normally used in clinical practice.

TABLE I. lists the values of the measured *Air-Kerma* by varying the tube voltage and the tube loading in the range 60-135 kV and 0.5-20 mA·s, respectively, which represent the typical values adopted in practice -ray analysis.

TABLE I. MEASURED K_{AIR} (mGy) VALUES OBTAINED VARYING TUBE VOLTAGE AND TUBE LOADING

$\begin{matrix} V \text{ (kV)} \\ Q \text{ (mAs)} \end{matrix}$	60	70	80	90	100	110	115	120	125	130	135
0.5	0.003	0.004	0.006	0.007	0.009	0.011	0.012	0.014	0.015	0.016	-
0.6	0.004	0.006	0.007	0.009	0.011	0.014	0.015	0.017	0.019	0.020	0.022
0.8	0.005	0.007	0.008	0.012	0.014	0.017	0.019	0.021	0.023	0.025	0.027
1.0	0.006	0.009	0.011	0.014	0.017	0.021	0.024	0.025	0.028	0.030	0.033
1.6	0.010	0.014	0.017	0.021	0.027	0.032	0.037	0.039	0.043	0.047	0.050
2.0	0.012	0.017	0.021	0.027	0.033	0.040	0.045	0.049	0.054	0.056	0.062
3.2	0.019	0.027	0.033	0.042	0.051	0.063	0.071	0.077	0.084	0.089	0.096
5.0	0.030	0.042	0.051	0.066	0.080	0.097	0.110	0.119	0.128	0.138	0.150
8.0	0.047	0.067	0.082	0.105	0.128	0.154	0.175	0.189	0.204	0.219	0.238
10.0	0.059	0.083	0.103	0.130	0.161	0.193	0.218	0.236	0.254	0.272	0.297
20.0	0.118	0.165	0.203	0.260	0.318	0.384	0.433	0.469	0.505	0.540	0.592

The obtained results shown that the K_{air} is linearly dependent on tube loading (as shown in Fig. 1 and that the coefficients of the linear regression vary with the tube voltage values as follows:

$$D_{air} = c_{1_{Vi}} \cdot Q + c_{2_{Vi}} \quad (1)$$

Unfortunately, these coefficients can change over time and with the continuous use of the x-ray device, so it is recommended to periodically verify the stability of the system performance.

The obtained relative mean root square fitting error is resulted to be over than 5.4 % for all tube voltage values considered.

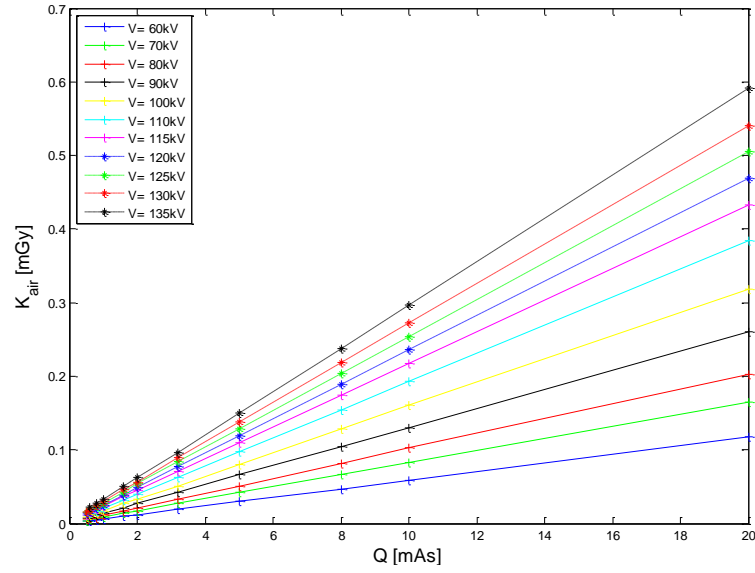


Fig. 1 Air-Kerma measurement as function of the tube loading for different tube voltage values

Moreover, for a fixed tube loading value, K_{air} can be expressed as quadratic function of tube voltage (as shown in Fig. 2) by providing a relative suitable mean root square fitting algorithm, whose error is resulted to be lower than 4%. These results confirm the good fitting of the proposed models assuring both the reliable of the x-ray device and the and validity of the tests.

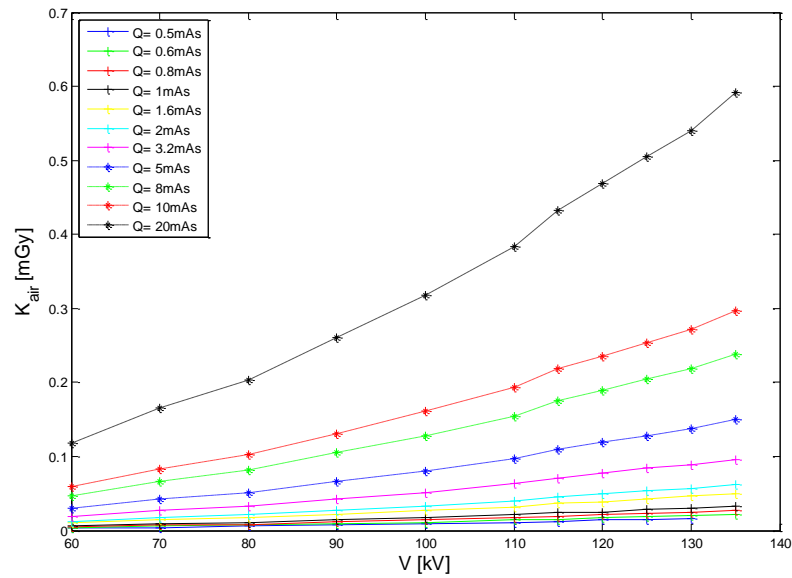


Fig. 2 Air-Kerma measurement as function of tube voltage for different tube loading values

B PHANTOM TOR CDR

After the modelling phase was completed the performance assessment of radiographic systems was carried out by means of TOR CDR (Leed Test Object).

TOR CDR consists on a plane sheet of perspex and metal including a set of standard objects designed to evaluate contrast and resolution.

Measurement tests for high and low contrast evaluation were performed by using two arrays having both 17 circular objects placed on TOR CDR. In particular, the first array consists of small disks with a diameter of 0.5 mm and high nominal contrast values varying in decreasing order. The second array includes large disks having a diameter of 11 mm and low nominal contrast values varying in decreasing order. TABLE II. list the relative nominal contrast values for all disks; these values have been calculated as relative intensity difference to the background for beam condition of 70 kV.

TABLE II. NOMINAL HIGH CONTRAST VALUES FOR DISCS WITH 0.5 MM DIAMETER

Disc Number	Nominal Contrast	Disc Number	Nominal Contrast
1	95.4 %	10	16.7%
2	82.0%	11	12.8%
3	72.6%	12	11.7%
4	57.3%	13	8.8%
5	49.6%	14	6.7%
6	36.0%	15	6.1%
7	30.2%	16	4.5%
8	23.8%	17	3.9%
9	20.3%		

TABLE III. NOMINAL LOW CONTRAST VALUES FOR DISCS WITH 11 MM DIAMETER

Disc Number	Nominal Contrast	Disc Number	Nominal Contrast
1	7.5%	10	1.5%
2	6.7%	11	1.3%
3	5.3%	12	1.1%
4	4.5%	13	0.9%
5	3.9%	14	0.7%
6	3.2%	15	0.5%
7	2.7%	16	0.3%
8	2.2%	17	0.2%
9	1.7%		

After the phantom is imaged, the elaboration software counts the number of circular details which are distinguished from background providing the threshold contrast for the radiographic device under test. This value depends on both the exposure conditions and the level of radiographic noise. Then, the elaboration software provides the value of Contrast-to-Noise Ratio (CNR) for each detected detail by means of the following expression:

$$CNR = \frac{\mu_d - \mu_b}{\sigma_b} \quad (2)$$

where μ_d and μ_b are the mean pixel value of detail and of the background, respectively, and σ_b is the standard deviation of pixel values of background [21].

Fig 3 shows the layout of TOR CDR test objects.

Measurement tests for the evaluation of the spatial resolution were performed by means of a set of 30 groups of bar patterns each comprising 5 radio-opaque bars and 4 radiolucent spaces with different spatial frequencies varying in increasing order and expressed as line pair per unit of distance (lp./mm).

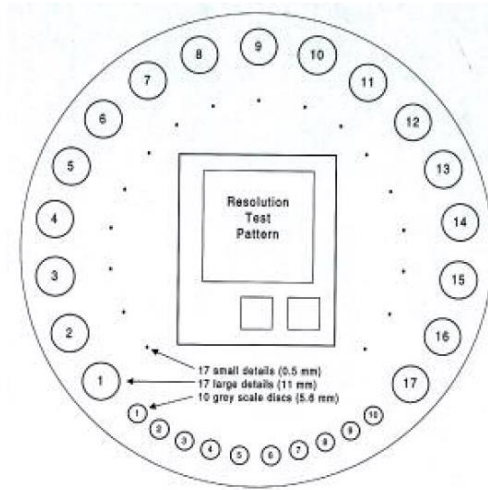


Fig. 3 Layout of TOR CDR test details [24]

In TABLE IV. the spatial frequency values for all bar patterns are reported.

TABLE IV. SPATIAL FREQUENCY VALUES FOR BAR PATTERNS

Group Number	Spatial freq. [lp./mm]	Group Number	Spatial freq. [lp./mm]
1	0.50	16	2.80
2	0.56	17	3.15
3	0.63	18	3.55
4	0.71	19	4.00
5	0.80	20	4.50
6	0.90	21	5.00
7	1.00	22	5.60
8	1.12	23	6.30

9	1.25	24	7.10
10	1.40	25	8.00
11	1.60	26	8.90
12	1.80	27	10.0
13	2.00	28	11.1
14	2.24	29	12.50
15	2.50	30	14.30

After the test pattern is imaged, the elaboration software counts the number of bar patterns which are visible providing the highest spatial frequency that can be resolved by the radiographic device under test.

The resolution limit is an indicator of radiographic unsharpness which is fully specified by Modulation Transfer Function (MTF). Fundamentally, this parameter measures the contrast ratio between input and output for different spatial frequencies and then empathizes the capability of distinguishing structures of different sizes. The elaborating software calculates the MFT for all resolved bar patterns by means of the following set of expressions based on the technique developed by Droegeand-Morin [25]:

$$MTF(f) = \begin{cases} \frac{\pi\sqrt{2}}{4} \cdot \frac{M(f)}{M_0} & \text{if } f \geq f_c / 3 \\ \frac{\pi\sqrt{2}}{4M_0} \cdot \sqrt{M^2(f) - \frac{M^2(3f)}{9} - \frac{M^5(5f)}{25} - \frac{M^7(7f)}{49}} & \text{if } f \geq f_c / 11 \end{cases} \quad (3)$$

$$\begin{cases} M(f) = \sqrt{\sigma_D^2 - N^2}; \\ M_0 = |\mu_r - \mu_b| \cdot \sqrt{\frac{n_r \cdot n_b}{n_r - n_b}}; \\ N^2 = \frac{\sigma_r^2 + \sigma_b^2}{2} \end{cases}$$

where σ_D is the standard deviation of pixel values inside the bar pattern region (detail) and μ_r is the mean pixel value bars in the reference region, respectively. In (3), σ_r and σ_b represent the standard deviation of pixels inside the bars reference and the background regions, respectively, and n_r and n_b are the number of pixels inside the bars reference and background regions. Finally, f_c represents the spatial frequency of the bar pattern.

C .EXPERIMENTAL TESTS

To evaluate the image quality performance of the analyzed radiographic system the phantom TOD CDR was placed as close as possible to the receptor with a focus to receptor

distance of 2 m, according to the Protocols for the assessment of Quality Image of Radiography Systems [26].

Then, the phantom was exposed to x-rays generated by ten different increasing tube potentials used in the characterization phase proposed in Section III.A. All resulting images were processed by means of the available elaboration software AutoPIA (*Automatic Phantom Image Analysis*) [27] which provides the values of *MTF* and *CNR* for high and low contrast details as function of changing in x-ray parameters values.

The experimental tests have been carried out by enabling the *Automatic Exposure Control*. As it known, the voltage increment produces a greater capacity to x-ray penetration resulting in exposure increasing. Therefore, when the *AEC* is switched on, increasing changes in tube voltages must be compensated by corresponding decreasing in tube loadings to maintain the same exposure.

For each value of tube voltage set during the tests the *AEC* system provides automatically a tube loading value whereas *Air-Kerma* is evaluated by (1).

TABLE V. shows the values of x-ray parameters used in the experimental tests, where *EI* represents the *Exposure Index* provided by Kodak radiographic device which is related to the incident exposure *X* by means of the following relationship [28]:

$$EI = 1000 \cdot \log_{10} X + 2000 \quad (4)$$

For Kodak digital x-ray device the typical exposure values in all radiographic exams range in 1500-1800 mR [29].

TABLE V. X-RAY PARAMETERS FOR FOR EXPERIMENTAL TESTS PERFORMED WITH AEC ON

	Image 1	Image 2	Image 3	Image 4	Image 5	Image 6	Image 7	Image 8	Image 9	Image 10
Tube voltage (kV)	60	70	80	90	100	110	120	125	130	135
Tube loading (mAs)	11,2	6	3,5	2,2	1,6	1,2	0,9	0,9	0,9	0,9
<i>K_{air}</i> (μGy)	66.1	50.0	36.2	29.4	26.6	24.7	23.3	25.7	27.5	29.6
<i>EI</i> (mR)	1800	1790	1790	1800	1770	1730	1780	1790	1790	1810

The results of experimental tests have been analyzed to correlate the x-ray parameters variation with quality performances.

It is possible to note that even in *EI* remains almost constant, the dose to air varies greatly with tube voltage changes by proving that the *Exposure Index* provided by the radiographic system should be not used as an indication of absorbed dose by the patient.

In particular experimental results show that *Air-Kerma* value decreases with reducing in tube loading despite increasing in tube voltage. Therefore the quantity of photons generated in the tube affects K_{air} more than the penetration energy of the photons. This result is in agreement with different studies [7], [30], [31] which have showed how K_{air} declines with tube voltage when imaging conditions are adjusted by *AEC* to achieve a similar exposure to receptor.

The minimum value of K_{air} is obtained for tube voltage of 120 kV. For tube voltage greater than 120 kV the *AEC* is not able to reduce tube loading which reaches the saturation point (about 0.9 m·As) with a consequent *Air-Kerma* increment due to growing in the voltage tube.

Fig. 4 shows the behavior of *MTF* as function of spatial frequency for ten different values of tube voltage. It is evident that changes in x-ray parameters slowly affect *MTF*; therefore the highest resolution limit (4 lp./mm) is obtained for low tube voltage, and it gets worse and worse (3.15 lp./mm) when the tube voltage increases.

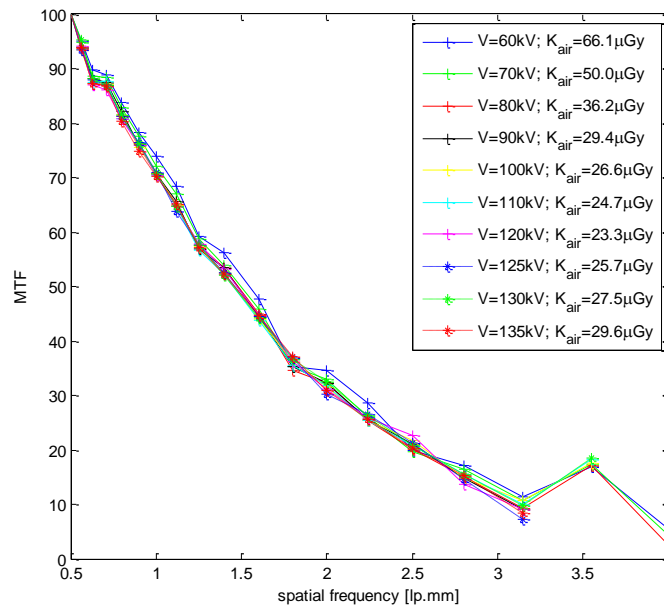


Fig. 4 *MTF versus spatial frequency for different tube voltages*

The *CNR* behavior for both high and low contrast details is more sensitive to changes in the tube voltage values (as shown in Fig. 5 and Fig. 6). In particular, best performance is obtained for lowest tube value which however provides high *Air-Kerma*. Therefore both K_{air} and *CNR* decline with tube potential; then, to obtain parameters setting that optimize the image quality, it

is necessary to find the best balance between an adequate quality level and a dose as low as possible.

To this aim the behavior of CNR versus K_{air} has been investigated. The analysis was limited to tube voltage up to 120 kV representing the threshold value beyond which the negative effect of decreasing in quality image and increasing in dose occurs. Moreover for tube voltage greater than 120 kV the threshold contrast detectable is reduced.

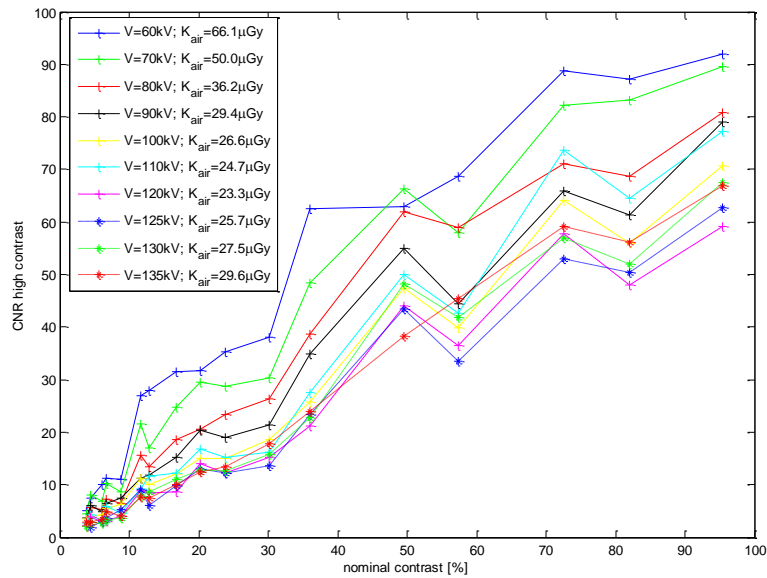


Fig. 5 CNR for high contrast details versus nominal contrast for different tube voltage values

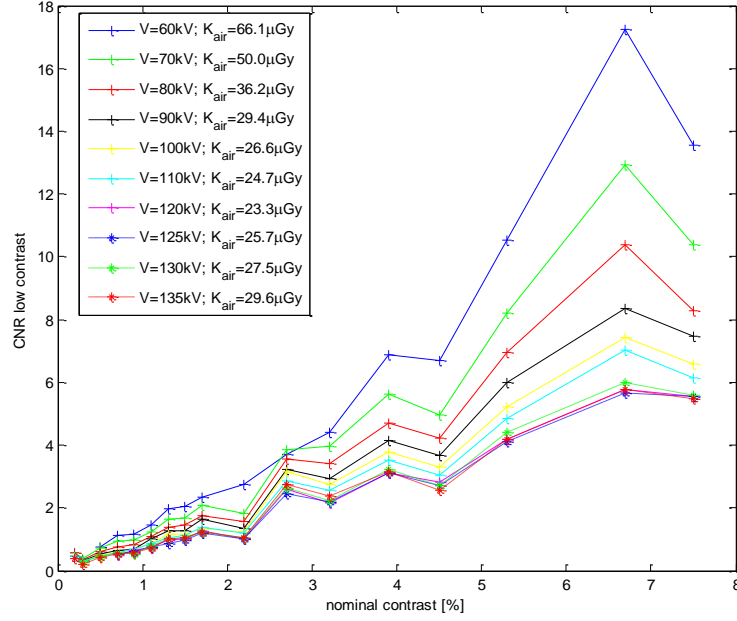


Fig. 6 CNR for low contrast versus nominal contrast for different tube voltage values

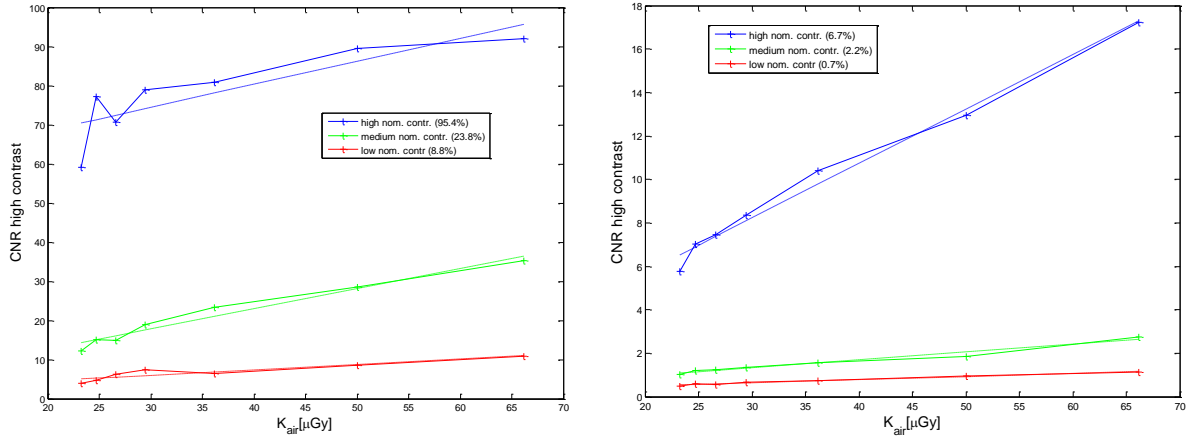


Fig. 7 CNR (a) high and (b) low contrast versus K_{air} for different nominal contrast

Fig. 7 (a) and (b) show the behavior of *CNR* (high and low contrast) as function of *Air-Kerma* values measured for disk details with high, medium and low nominal contrast. It is possible to note that *CNR* is less sensitive to *Air-Kerma* variations for objects having low nominal contrast. To evaluate the sensitivity of *CNR* versus K_{air} , the angular coefficients of regression lines of curves plotted in Fig. 7 (dash and dot lines) were calculated obtaining the values listed in TABLE VI.

TABLE VI. CNR HIGH AND LOW CONTRAST SENSITIVITY FOR DIFFERENT NOMINAL CONTRASTS

High contrast-small details		Low contrast- large details	
<i>Sensitivity</i> [CNR/ μ Gy]	<i>Nominal contrast</i>	<i>Sensitivity</i> [CNR/ μ Gy]	<i>Nominal contrast</i>
0,59	95.4 %	0,25	6.7 %
0.51	23.8 %	0.03	2.7 %
0.14	8.8 %	0.01	0.7 %

Low contrast-large details are less sensitive to dose increasing with respect to the high contrast -small details.

Therefore, taking into account that the detectability of low contrast details is a crucial phase in x-ray exams and that the image quality for these details is not significantly improved with dose increasing, it is preferable use slightly large tube voltages (90-110 kV). In this case even if *CNR* on average decreases about 40%, the *Air-Kerma* value declines more than 60% reaching values lower than 30 μ Gy which fit the typical operating range provided in x-ray exams [31]. Moreover these tube voltage values provide very similar resolution limit and nominal contrast threshold with respect to lower tube voltage assuring a good details detectability.

The obtained results allowed studying the behavior of *CNR* and *MFT* as function of K_{air} so to identify correlation between image quality indexes and radiographic parameters. It is showed that in standard operating conditions and when *AEC* was used, greater attention must be paid to the choice of tube voltage setting; in particular the best balance between image quality and dose to air implies applying average tube voltage values.

IV. CONCLUSION

In the proposed work, an analysis of imaging performance of digital radiographic system was presented.

Digital x-ray systems can induce an excessive dose to the patient in the medical examinations. With this premise, an in-depth analysis is advisable to identify the optimal technical parameters to reduce the levels exposure and to assure a suitable image quality. The experimental tests based on the use of Leed Test Object allow identifying the correlation between the radiation dose and the main radiographic parameters such as to obtain a fixed image contrast level.

Acknowledgment

The Authors wish to thank the clinicians of Hospital of “Casa del Solievo della Sofferenza” of San Giovanni Rotondo, Apulia, Italy, for both providing the data necessary for the proposed study and for their helpful discussions.

REFERENCES

- [1] H. Hricak, D. J. Brenner, S. J. Adelstein, D. P. Frush, E. J. Hall, R. W. Howell, C. H. McCollough, F. A. Mettler, M. S. Pearce, O. H. Suleiman, J. H. Thrall, L. K. Wagner, “Managing Radiation Use in Medical Imaging: A Multifaceted Challenge”, *Radiology*, vol. 258, no.3 pp.889-905, 2011.
- [2] J.A Rowlands, “Current advances and future trends in X-ray digital detectors for medical applications,” *IEEE Trans. on Instrumentation and Measurement*, vol 47, no. 6 pp.1415–1418, December 1998.
- [3] F. Adamo, G. Andria, F. Attivissimo, A. M. L. Lanzolla, M. Spadavecchia, A comparative study on mother wavelet selection in ultrasound image denoising, *Measurement*, vol. 46, June 2013, pp. 2447-2456.
- [4] F. Attivissimo, G. Cavone, A. M. L. Lanzolla, M. Spadavecchia, A Technique to Improve the Image Quality in Computer Tomography, *IEEE Trans. on Instrumentation and Measurement*, vol. 59, no. 5, May 2010, pp. 1251-1257.
- [5] Z. Sun, C. Lin, Y.S. Tyan, K.H Ng, “Optimization of chestradiographic imaging parameters: a comparison of image quality and entrance skin dose for digital chest radiography systems,” *Clinical Imaging*, vol. 36, no. 4, pp. 279-286, July-August 2012
- [6] G. Andria, F. Attivissimo, A. Nisio, A.M.L.Lanzolla, G. Guglielmi, R. Terlizzi, “Dose Optimization in Chest Radiography: System and Model Characterization via Experimental Investigation”, *IEEE Transactions on Instrumentation and Measurement* 2013.
- [7] C.J. Martin, “Optimization in general radiography”, *Biomedical Imaging and Intervention Journal*, vol. 3, no. 2, , April 2007, pp. 1-18.
- [8] S. Balter, D. L. Miller, E. Vano, P. Ortiz Lopez, G. Bernard, E. Cotelo, K. Faulkner, R. Nowotny, R. Padovani, A. Ramirez, “A pilot study exploring the possibility of establishing guidance levels in x-ray directed interventional procedures” *Medical Physics* vol.35 no.2, February 2008, pp. 673-680.
- [9] E. Samei, “Performance of DigitalRadiographic Detectors:Quantification and assessment Methods” *Advances in Digital Radiography: RSNA Categorical Course in Diagnostic Radiology Physics*, pp 37–47, 2003.
- [10] M. B. Williams, E. A. Krupinski, K. J. Strauss, W. K. Breeden, M. S. Rzeszutarski, K. Applegate, M. Wyatt, S. Bjork, J. A. Seibert, *Digital Radiography Image Quality:Image Acquisition*, American College of Radiology, pp.371-388, 2007.
- [11] V. Bhateja, M. Misra, S. Urooj, A. Lay-Ekuakille, “A Robust Polynomial Filtering Framework for Mammographic Image Enhancement from Biomedical Sensors”, *IEEE Sensors Journal*, vol.13, n.11, pp. 4147 – 4156, 2013
- [12] W. Muhogora, R. Padovani, P. Msaki, “Initial quality performance results using a phantom to simulate chest computed radiography”, *Journal of Medical Physics*, vol.36, no.1, Jan-Mar 2011, pp. 22-28.
- [13] S.ZhonghuaSun,L.Chenghsun,T.YeuSheng.Ng.Kwan-Hoong “Optimization of chest radiographic imaging parameters: a comparison of image quality and entrance skin dose for digital chest radiography systems”, *Clinical Imaging* ,vol. 36, 2012 pp. 279–286
- [14] A. R. Várkonyi-Kóczy “Low complexity situational models in image quality improvement” *Studies in Computational Intelligence*, vol, 372, 2011, pp. 155-177 .
- [15] C.J. Martin, P.F. Sharp, D.G. Sutton, “ Measurement of image quality in diagnostic radiology”, *Applied Radiation and Isotopes*, no 50, 1999, pp 21-38
- [16] A. R. Várkonyi-Kóczy “New advances in digital image processing” *Memetic Computing*, no. 4, vol. 2, December 2010, pp. 283-304

- [17] M. B. Williams, E. A. Krupinski, K. J. Strauss, W. K. Breeden , M. S. Rzeszutarski, K. Applegate, M. Wyattg, S. Bjork, J. A. Seibert, "Digital radiography image quality: Image acquisition," Amer. College Radiol., vol. 4, no. 6, pp. 371–388, 2007.
- [18] <http://www.rkymtnrad.com/pdfFiles/DR7500.pdf>
- [19] L. Bowden, R. Faulkner, C. Clancy, A. Gallagher, M. Devine, D. Gorman , G. O'Reilly, A. Dowling. "Doses under automatic exposure control (AEC) for direct digital radiographic (DDR) X-ray systems", Radiation Protection Dosimetry , vol. 147, no 1-2, September 2011.
- [20] "European protocol for the quality control of the physical and technical aspects of mammography screening" European guidelines for quality assurance in breast cancer screening and diagnosis Fourth edition, 2006.
- [21] J. T. Bushberg, J. A. Seibert, E. M. Leidholdt Jr, J. M. Boone, "The Essential Physics of Medical Imaging", 2011 Lippincott Williams & Wilkins.
- [22] F. M. Khan, J.P. Gibbon, "The Physics of Radiation Therapy", 2014 Lippincott Williams & Wilkins
- [23] <http://www.rti.se/products/piranha/>
- [24] <http://www.leedstestobjects.com/>
- [25] R.T. Droege, R.L. Morin "A practical method to measure the MTF of CT scanners" Med Phys. vol 9, no.5, pp. 758-760, September-October 1982.
- [26] International Commission on Radiological Protection, Managing patient dose in digital radiology, Annal of ICRP, Publication 93, vol 34 , no. 1, pp. 1-73, 2004.
- [27] <http://autopia.cyberqual.it/index.php/AutoPIA>
- [28] American Association of Physicists in Medicine (AAPM), An Exposure Indicator for Digital Radiography, Report no. 116, July 2009.
- [29] CRCPD's H-33 Task Force for the Inspection Protocol of Diagnostic X-ray Facilities using CR/DR Technology "Computed radiography (CR) and Digital radiography (DR) state x-ray inspection protocol" Conference of Radiation Control Program Directors, Inc. , January 2010
- [30] C.J. Martin "The importance of radiation quality for optimization in radiology" Biomedical Imaging and Intervention Journal, vol. 3, no. 2, April 2007, pp. 1-18.
- [31] N.M. Marshall "An examination of automatic exposure control regimes for two digital radiography systems" Physic Medicine and Biology , vol. 54, 2009, pp. 4645-4670.